Evaluation of vacuum contactor testing facility by optical and spectroscopic investigations

C. Vitelaru[1], A. Radulian[2], N. Mocioi[2], V. Braic[1]

[1]National Institute for Optoelectronics-INOE 2000, 409 Atomistilor Str., 077125, Magurele, Romania
[2]ICPE, 313 Splaiul Unirii Str., 030138, Bucuresti, Romania

Optical Emission Spectroscopy and fast imaging were performed in a testing facility designed to measure electrical characteristics of vacuum contactors. The emission spectra are used to identify the dominant species in the discharge volume between electrodes, depending on the current regime. The fast imaging offers a global view on the temporal and spatial evolution of the arcs developing between the two electrodes. Moreover the mechanical movement of the mobile electrode is quantified and analysed, in relation with the electrical measurements.

1. Introduction

Vacuum arcs, sustained in metal vapor of the contact electrodes, occur in vacuum contactors after disconnecting of an inductive load. Due to the vacuum arc instability there can be a current drop to zero before the natural zero crossing of the sinusoidal waveform of the current. If the value of *chopping* current is too high, this fast variation of the current along with circuit impedance can produce overvoltages **[1]**. The general requirements for contact material are: high electrical and thermal conductivity, arc erosion resistance, high mechanical hardness, dielectric strength, braking capacity and dielectric recovery **[2]**. Some specific requirements should be added, such as minimal gas content, low thermo-ionic emission, low vapor emission, optimum metal vapor pressure, to ensure low chopping current values Comprehensive testing of chopping current behavior is therefore necessary before using a certain material as contact material. **[3]**.

2. Experimental part

2.1. Experimental Setup

The electrical circuit of the test facility that measures the copping current under specific conditions is shown in Fig.1. A synthetic circuit produces a current pulse with an amplitude up to 100A at a supply frequency of 50 Hertz, The opening motion of the electrical contacts is produced by an electro-mechanical actuator after the current pulse was applied to them. At the begining of the separation of the electrical contacts it appears a diffuse arc that becomes unstable and the current is quickly chopping to zero. The waveform of the chopping current is recorded using a coaxial shunt and an oscilloscope. The parameters of the testing system are: opening movement proper time is ~ 7ms, average speed of the moving contact of 1.2 m/s (can be adjusted by spring contact pressure), distance between contacts 2-3 mm. The electrical contacts are mounted in a vacuum chamber where the pressure level is 10^{-7} mbar.

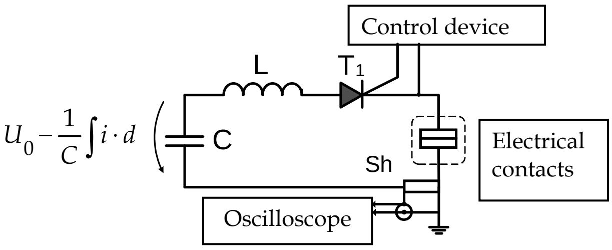

Fig.1 Electrical circuit of the chopping current measuring unit

The optical emission spectroscopy of the arc discharge occurring between the two electrodes was performed by using a portable Ocean Optics USB2000 spectrometer. The spectra were acquired in the 200 to 900 nm wavelength interval, with an acquisition time longer than the specific discharge period. The information thus obtained is time and space averaged, allowing only identifying the dominant species present in the discharge volume.

Fast imaging measurements were performed to globally characterize the emissivity of the discharge created between the two electrodes. For this purpose a Motion Pro X3 fast acquisition camera was used, with typical acquisition frequency of 1000 fps at 1024x1280 pixel resolution and maximum frequency of 64000 fps.

2.2. High current regime

The experimental procedure of the contacts testing starts with a first high current phase, necessary for conditioning the electrodes surface. At this stage the maximum current intensity injected into the system is on the order of 1 kA, this high value being necessary to evaporate all the unwanted compounds that might be found on the target surface. A typical emission spectrum of such a high current regime is represented in Fig. 2, along with some of the main emission lines that were identified **[4]**. The spectrum is dominated in this case by the W atoms and ions, showing that an efficient removal of all species on the target is performed (including the ones with lower evaporating yield). The Ag lines are also present, but they are rather small compared with the ones corresponding to tungsten.

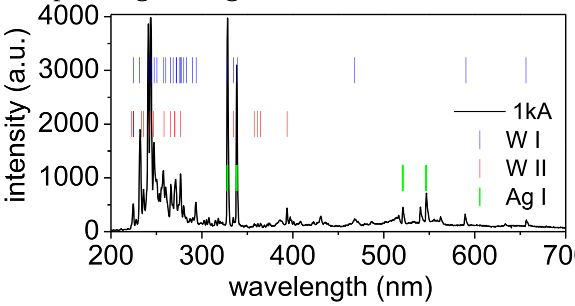

Fig2. Typical emission spectrum during the conditioning phase of WC/Ag (60%/40%) contacts, at 1 kA maximum current intensity

Emission spectra were acquired for different discharge conditions, showing the same trends as the ones already described. As the spectra are completely time and space averaged no information on spatial distribution or temporal behavior could be extracted.

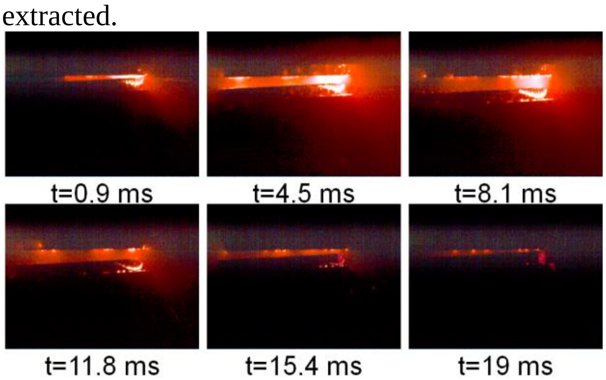

Fig3. Images of the discharge between two WC/Ag electrodes under high current conditions (1.26 kA), at various time intervals

The fast imaging on the other hand, can give valuable information on the spatial and temporal distribution of the discharge regions. Therefore, six representative images are presented in Fig.3, obtained during the conditioning stage of the electrodes (20 ms typical duration of discharge, maximum current intensity 1.26 kA). The parameters used for the camera were: acquisition rate 2200 fps, 100 μs exposure time. There were fifty images acquired during 22.7 ms time of discharge, only six of them being represented in Fig.3. A red filter was used to acquire the images, to reduce the light intensity (especially in the UV domain) and to avoid image saturation when using the needed exposure times.

The first image on Fig.3 (top left) shows that after 0.9 ms from initiating the electrode movement there is an intense bright region in the right side of the image. A large number of micro-particles were ejected from this region, their trajectory being visible by the bright lines going towards the low right corner of the image. The emission inhomogeneity is kept for most of the following images. Moreover, on the mobile electrode, lower side of the image, there is an agglomeration of large size, low velocity particles. This corresponds to a preferential evaporation area on the electrodes surface, which was observed after experiments ending. The images obtained towards the end of the recording (19 ms) show the presence of low intensity micro-arcs, accompanied by a much lower number of micro-particles.

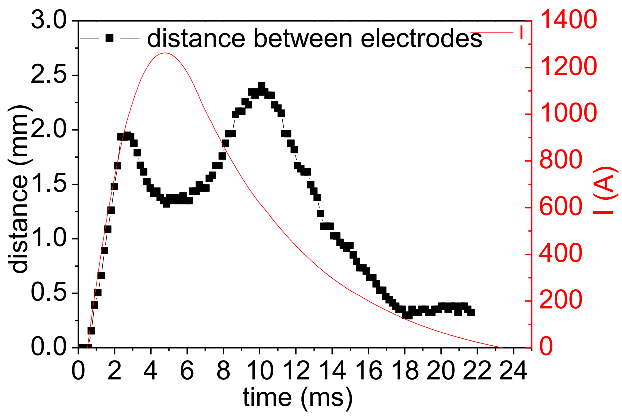

Fig 4. Time evolution of distance between electrodes and current intensity, when opening WC/Ag contact in high current regime (electrode forming)

The preliminary analysis of the images showed that electrode movement is not uniform. A more detailed analysis of the movement was performed by using a higher acquisition rate (5540 fps), obtaining images with a time step of 180 μs. By digitally processing the images one can measure the distance between electrodes for each image, the time evolution of this distance being represented in Fig 4. The current intensity time evolution is represented in the same figure. A few stages of the contactor opening can be identified, as follows: (i) the first opening stage, synchronous with the current intensity increase, in the first 2 ms, with a mobile contact velocity of 1 m/s; (ii) an oscillatory phase, taking about 8 ms. The electrodes are first approaching to a minimum distance of ~1.3 mm and then drive away to a maximum distance of ~2.4 mm; (iii) an exponentially decay with a 5.6 ms time constant; (iv) a stationary phase were the contacts remain fixed at 0.3 mm from each other. From this analysis results that the distance between electrodes has a complex time behavior, influencing the arc development when opening the contact.

2.3. Chopping current regime

The second part of the contact testing consists in measuring the current intensity evolution when opening the circuit, at maximum current intensity values close to the ones to be used in the final application. In Fig. 5 there are 34 current intensity curves, registered in similar conditions for WC/Ag electrodes. The inset shows the current distribution at the end of the pulse, where the chopping current can be measured. In this case the registered values for the chopping current range between 0.3 and 0.8 A. Let us note that the desired low value of the chopping current is obtained by maintaining the discharge in the volume as long as possible. On the other hand, under normal operating conditions, the discharge should not be reignited on the increasing part of alternative applied voltage. Since the testing facility only reproduces the interruption of the current flow, these aspects will not be discussed here.

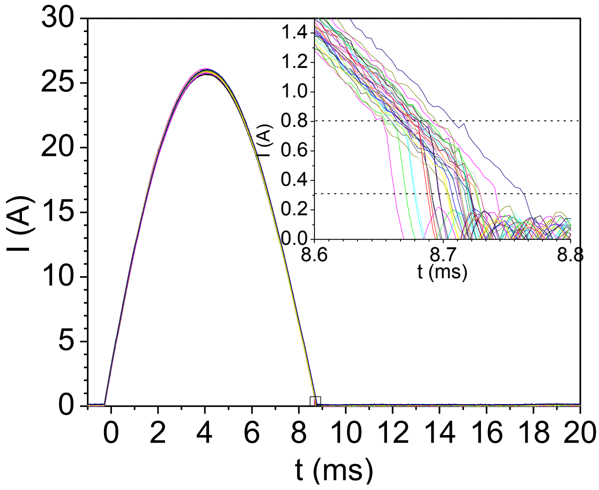

Fig.5 Time evolution of current intensity when opening the WC/Ag contacts, for typical conditions of measuring the chopping current (I_{max}=25 A)

Same as for the high current regime, emission spectra were acquired during the chopping current measurement. A typical spectrum is represented in Fig.6, together with the emission lines identified and marked with vertical lines. By comparing it with the spectrum in Fig. 2, one can see that the dominant lines now are belonging to Ag, the W emission line being less intense. For these conditions therefore, which are closer to the working conditions of the future vacuum contactor, the discharge is maintained mainly in the vapors of the easily fusible material (Ag in this case). Emission spectra were acquired for most of the registered curves in Fig. 5 but no direct connection between the chopping current and the evolution of emission lines could be found. This was due mainly to the lack of spatial or temporal resolution. Further developments of the method, namely time resolved measurements focused on the emission lines identified here, are necessary to investigate such a correlation.

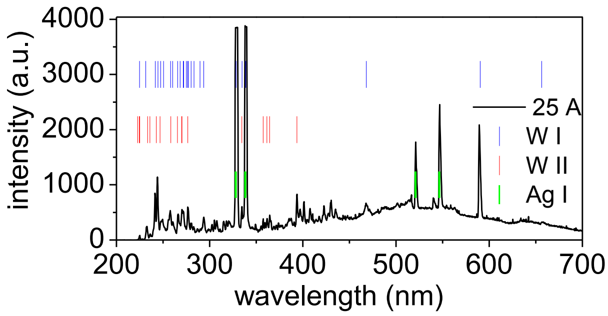

Fig 6 Typical emission spectrum during the measurement of chopping current of WC/Ag (60%/40%) contacts, at 25 A maximum current intensity

The spatial and temporal behaviour of the discharge developing between electrodes was also investigated, by fast imaging. For these conditions with lower light intensity, due to much lower current, no filter was used and the amplification facility of the camera was used to acquire satisfactory images. The acquisition rate was 2000 fps (0.5 ms time step between images) and exposure time was 497 μs.

Six representative images are presented in Fig. 7, at different time intervals during the opening of the contact. These images confirm that there is a preferential ignition of the arcs on the right side of the image. These micro arcs lead to the evaporation of metal atoms (which were identified by emission spectroscopy in Fig.2 and 6), and also to the ejection of micro particles. One of these micro-particles can be distinctively identified in each image, and is marked by the red circles. Each individual image shows the path of the particle during the acquisition time (497 μs). The selected images show, as follows: (i) the reflection on the upper electrode (t=3.5 ms); (ii) the movement towards the lower electrode (t=4 and 5.5 ms); (iii) the touch of the lower electrode (t=6 ms); (iv) the movement towards the outer part of the electrodes (t=6.5 and 8ms). It is interesting to notice that the particle can be present in the volume even after the complete extinguish of the arcs, being a possible trigger for the re-ignition and interruption failure in the real contactor. It is therefore important to be able to follow and describe the trajectory and distribution of these particles.

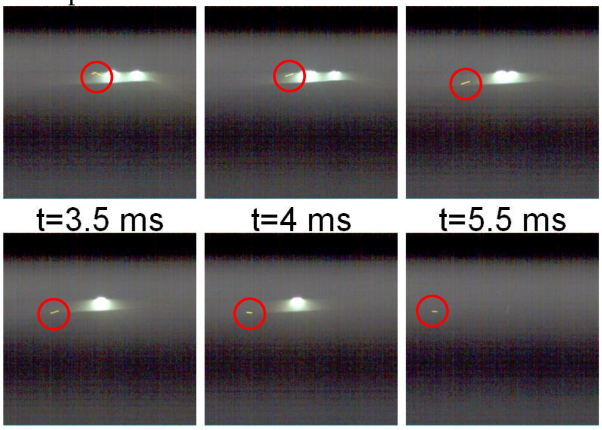

Fig 7. Images of the discharge between two WC/Ag electrodes when measuring the chopping current (25 A), registered at different time intervals

The trajectory of the particle was extracted from the detailed analysis of all the images corresponding to the series in Fig. 7, and is represented in Fig.8. The trajectory shows the exact stages of the movement described for Fig.7. Moreover, the velocity of the particle can be derived, as being the size of the light trace divided by the acquisition time. The average velocities obtained indicate that the particle is moving with 2.43 mm/s before collision with the surface, and with a lower velocity (1.37 mm/s) after changing the direction.

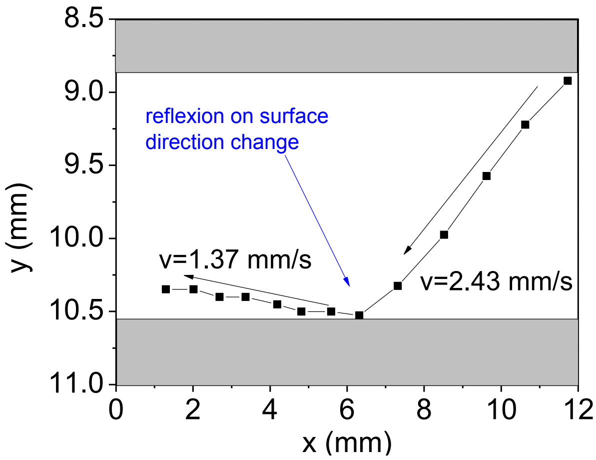

Fig 6. Real trajectory of the micro-particle identified by red circles in Fig. 7

2.4 Conclusions and perspectives

The characterization of the vacuum contactor testing facility by optical methods gives a good insight on both technological issues, and the fundamental processes occurring in the discharge region. The emission lines identified by emission spectroscopy allowed identifying the arc evaporated elements, in different discharge conditions. Further developments, time and space resolved measurements, are necessary to allow a direct comparison of electrical and optical parameters.

The fast imaging technique, allowed the description off different mechanical characteristics, such as inhomogeneity due to mechanical movement, preferential localized evaporation, spatio-temporal behavior of mobile electrode, etc. The information thus obtained by such a non-intrusive technique can serve for fixing and testing some parameters, such as velocity of opening contacts, total duration, distance between electrodes, etc.

Another type of analysis, using fast imaging, refers to the identification and description of micro particles, in terms of trajectory, velocity, distribution, etc. Future developments can include a comparison of these characteristics in different conditions, such as different electrode materials and/or erosion degree, maximum current value, velocity of opening contacts, etc.

Summarizing, the results obtained and presented so far allow the identification of possible routes of using the described techniques in the field of vacuum contactors Further developments are necessary to link the obtained information with the parameters relevant for the application, such as chopped current, stability in time, domain of use, etc.

Acknowledgment: Funding by the Romanian National Authority for Scientific Research, UEFISCDI, through project PN-II-PT-PCCA-34/2012, NeWaLC is acknowledged

3. References

[1] Slade, P., The Vacuum Interrupter: Theory, Design, and Application, Ed. CRC Press, New York, 2001;

[2] Grill, R., Kläusler, P., Mueller, F., Schrott, O., Hauser, H., WC / Ag Contact Materials with Improved Homogeneity, Plansee Seminar, 2005;

[3] Hortopan, G., Aparate electrice, Ed. Didactică şi pedagogică, Bucureşti, 1980;

[4] A. Kramida, Y. Ralchenko, J. Reader, **2013**, NIST ASD Team: Nist Atomic Spectra Database (version 5.0).